

UC Santa Cruz

UC Santa Cruz Previously Published Works

Title

Two-dimensional ^1H NMR studies of paramagnetic bimetallic mixed-metal complexes

Permalink

<https://escholarship.org/uc/item/5v5925xm>

Journal

Magnetic Resonance in Chemistry, 31(13)

ISSN

0749-1581

Authors

Wang, Zhigang

Holman, Theodore R

Que, Lawrence

Publication Date

1993-12-01

DOI

10.1002/mrc.1260311316

Copyright Information

This work is made available under the terms of a Creative Commons Attribution License, available at <https://creativecommons.org/licenses/by/4.0/>

Peer reviewed

Two-Dimensional ^1H NMR Studies of Paramagnetic Bimetallic Mixed-Metal Complexes

Zhigang Wang, Theodore R. Holman and Lawrence Que, Jr*

Department of Chemistry, University of Minnesota, Minneapolis, Minnesota 55455, USA

Synthetic dinuclear mixed-metal complexes have proved useful as models for metal-substituted dinuclear iron-oxo proteins. However, a detailed assignment of their paramagnetically shifted proton NMR resonances has thus far been difficult to achieve. In the light of the significant role of two-dimensional (2D) NMR techniques in establishing the bond connectivities in diamagnetic molecules, COSY studies were performed on a series of complexes, $[\text{Fe(II)M(II)BPMP}(\text{O}_2\text{CCH}_2\text{CH}_3)_2]^+$ {BPMP = 2,6-bis[bis(2-pyridylmethyl)aminomethyl]-4-methylphenol, M = Mn, Co and Zn}, taking advantage of the short electronic relaxation time of Fe(II). The resonances from the four distinct pyridine rings of each of the three complexes were unambiguously assigned based on the bond-correlated cross signals in the 2D spectra due to the (α)- β - γ - β' pyridyl proton connectivities. The resonances from the two bridging ligands of these complexes were also unambiguously assigned based on the same approach. Together with longitudinal relaxation time (T_1) measurements, the 2D data allow the assignment of all the paramagnetically shifted proton resonances of all the three bimetallic complexes.

KEY WORDS ^1H NMR 2D NMR Mixed-metal complexes Non-haem iron

INTRODUCTION

Dinuclear iron-oxo centres have been found in the active sites of several metalloproteins,¹ including hemerythrin,² the R2 protein of ribonucleotide reductase,³ the hydroxylase component of methane mono-oxygenase,⁴ purple acid phosphatase^{5,6} and stearyl-acyl carrier protein Δ^9 -desaturase.⁷ An increasingly powerful method for studying the structures and functional roles of these diiron centres has been to replace one of the 'native' ions of the metalloproteins with a different metal to alter the spin physics of the dinuclear centre and thus modify the spectroscopic and biological properties of the active site.⁸⁻¹² However, the interpretation of the results from the spectroscopic and physical measurements on the metal-substituted proteins is complicated by the large number of interactions and permutations involved. The synthesis of small bimetallic mixed-metal model complexes which mimic the structure of the target biological active site thus affords a strategy to help sort out some of the complexity. By using the symmetrical dinucleating ligand 2,6-bis[bis(2-pyridylmethyl)aminomethyl]-4-methylphenol (HBPMP) to hold the two metal ions in close proximity via a μ -phenoxo bridge,¹³ we have developed a general synthetic route for preparing bimetallic mixed-metal complexes in which one of the metal centres is iron. This approach has afforded the complexes $[\text{Fe(III)Ni(II)BPMP}(\text{O}_2\text{CCH}_2\text{CH}_3)_2]^{2+}$, $[\text{Fe(III)Zn(II)BPMP}(\text{O}_2\text{CCH}_2\text{CH}_3)_2]^{2+}$ and $[\text{Fe(II)Ga(III)BPMP}(\text{O}_2\text{CCH}_2\text{CH}_3)_2]^{2+}$ ^{14,15} with one trivalent and one

divalent metal centre. The reduction of the Fe(III) centre in these Fe(III)M(II) complexes allows the synthesis of dinuclear complexes where both metal centres are divalent, i.e. $[\text{Fe(II)M(II)BPMP}(\text{O}_2\text{CCH}_2\text{CH}_3)_2]^+$ (M = Mn, Co, Zn).¹⁶⁻¹⁸

NMR spectroscopy has proved to be a very powerful technique for probing the coordination environments of the paramagnetic metal centres, owing to large paramagnetic shifts engendered by such centres.^{19,20} However, detailed assignments of the paramagnetically shifted proton NMR resonances, even for model complexes, have proved difficult because of uncertainties in proton-proton connectivities. Two-dimensional (2D) NMR techniques such as COSY and TOCSY provide such information²¹ and have recently been successfully applied to paramagnetic model complexes²²⁻²⁷ and metalloproteins.^{12,28-30} Examples include COSY, TOCSY and EXSY studies of the symmetric dinuclear iron-oxo model complexes, $[\text{Fe(II)Fe(II)BPMP}(\text{O}_2\text{P}(\text{OPh})_2)_2]^+$ and $[\text{Fe(II)Fe(III)BPMP}(\text{O}_2\text{P}(\text{OPh})_2)_2]^{2+}$,²⁷ and NOESY studies on the reduced purple acid phosphatase from porcine uterus whose Fe(II) site is substituted by Co(II).¹²

In this paper, we report 2D bond-correlation COSY studies and longitudinal relaxation time (T_1) measurements on a series of bimetallic mixed-metal model complexes, $[\text{Fe(II)M(II)BPMP}(\text{O}_2\text{CCH}_2\text{CH}_3)_2]^+$ (M = Mn, Co and Zn), where we identify the proton resonances from the four distinct pyridine rings and the two different propionate bridging ligands in these paramagnetic complexes. The results demonstrate that we can use the COSY technique to obtain valuable information about the structures of more complicated model complexes.

EXPERIMENTAL

Syntheses

All chemicals were of the highest grade available and used as received. The solvents CH_2Cl_2 and CH_3CN were distilled from CaH_2 under argon before use. Microanalysis were performed by Desert Analysis (Tucson, AZ, USA).

The ligand 2,6-bis[bis(2-pyridylmethyl)aminomethyl]-4-methylphenol (HBMPMP) was synthesized according to published procedures.¹³

(Bis- μ -*O*,*O'*-propionato)(2,6-bis[bis(2-pyridylmethyl)aminomethyl]-4-methylphenolato)iron(II) manganese(II) tetraphenylborate, [Fe(II)Mn(II)BPMP($\text{O}_2\text{CCH}_2\text{CH}_3$)₂]BPh₄ (1). [Fe(II)-Mn(II)BPMP($\text{O}_2\text{CCH}_2\text{CH}_3$)₂]BPh₄ was prepared by reducing [Fe(III)Mn(II)BPMP($\text{O}_2\text{CCH}_2\text{CH}_3$)₂](BPh₄)₂.¹⁷ Briefly, 1.1 equiv. of cobaltocene was added to a solution of [Fe(III)Mn(II)BPMP($\text{O}_2\text{CCH}_2\text{CH}_3$)₂](BPh₄)₂ (0.03 g, 0.019 mmol) in 3 ml of CH_3CN under anaerobic conditions. The purple solution rapidly changed to yellow–orange, indicating that reduction of the complex had occurred. On standing, a yellow precipitate appeared; this was filtered, washed with methanol and recrystallized from CH_2Cl_2 – CH_3CN to afford light-orange crystals.

(Bis- μ -*O*,*O'*-propionato)(2,6-bis[bis(2-pyridylmethyl)aminomethyl]-4-methylphenolato)iron(II)cobalt(II) tetraphenylborate, [Fe(II)Co(II)BPMP($\text{O}_2\text{CCH}_2\text{CH}_3$)₂]BPh₄ (2). The precursor [Fe(III)Co(II)BPMP($\text{O}_2\text{CCH}_2\text{CH}_3$)₂](BPh₄)₂ was synthesized according to the following procedures. A solution of 0.1 g (0.19 mmol) of HBMPMP in 10 ml of methanol was treated with a solution of 0.076 g (0.19 mmol) of $\text{Fe}(\text{NO}_3)_3 \cdot 9\text{H}_2\text{O}$ in 5 ml of methanol to yield a dark-blue solution, which contains the mononuclear iron complex. Sequential addition of 47 ml (0.19 mmol) of $\text{Co}(\text{NO}_3)_2$ (4 M aqueous solution), 0.055 g (0.57 mmol) of sodium propionate in 5 ml of methanol and a methanolic solution of sodium tetraphenylborate (0.27 g, 0.76 mmol) afforded the crude product, which was filtered through a medium-fritted glass filter. Further purification was achieved by recrystallization of the crude product by vapour diffusion of methanol into an acetone solution of the complex.

[Fe(II)Co(II)BPMP($\text{O}_2\text{CCH}_2\text{CH}_3$)₂]BPh₄ was then prepared by adding 1.1 equiv. of cobaltocene to a solution of [Fe(III)Co(II)BPMP($\text{O}_2\text{CCH}_2\text{CH}_3$)₂](BPh₄)₂ (0.03 g, 0.019 mmol) in 3 ml of CH_3CN under anaerobic conditions. The color of the solution rapidly changed to orange, indicating that reduction of the complex had occurred. On standing, a light-orange precipitate appeared; this was filtered, washed with methanol and recrystallized from CH_2Cl_2 – CH_3CN to yield light-orange crystals. Owing to some scrambling during the recrystallization process, small amounts of Fe(II)Fe(II) and Co(II)Co(II) complexes were found in the product, as judged from the NMR spectrum.

(Bis- μ -*O*,*O'*-propionato)(2,6-bis[bis(2-pyridylmethyl)aminomethyl]-4-methylphenolato) iron(II)zinc(II) tetraphenylborate, [Fe(II)Zn(II)BPMP($\text{O}_2\text{CCH}_2\text{CH}_3$)₂]BPh₄ (3). [Fe(II)Zn(II)BPMP($\text{O}_2\text{CCH}_2\text{CH}_3$)₂]BPh₄ was synthesized as reported previously.¹⁸ Small amounts of Fe(II)Fe(II) and Zn(II)Zn(II) complexes were found in the Fe(II)Zn(II) samples because of metal site scrambling during the recrystallization process.

Spectra

1D ¹H NMR spectra and ¹H *T*₁ values were measured on a Varian VXR300 NMR spectrometer at 299.949 MHz at room temperature. The spectra were obtained using a 90° pulse with 16K data points and 2000 transients. Chemical shift values are reported relative to TMS with positive values indicating downfield shifts. Signal-to-noise ratios were improved by using a line-broadening factor of 30 Hz in the Fourier transformation. An inversion–recovery pulse sequence (180°– τ –90°–AQ) was used to obtain non-selective proton longitudinal relaxation times (*T*₁) with the

carrier frequency set at several different positions to ensure the validity of the measurements.

2D ¹H NMR data were collected on a Varian VXR500 instrument at 499.843 MHz at room temperature. A typical magnitude COSY spectrum were obtained by collecting 1024 data points in *t*₂ and 256 data points in *t*₁ with a repetition time of <0.1 s. The time for the data collection for a saturated sample was about 12 h. A 0° shifted sine bell combined with a Gaussian function was applied in both dimensions and zero-filled to 2048 (*t*₂) × 2048 (*t*₁) data points prior to Fourier transformation and symmetrization.

RESULTS AND DISCUSSION

The crystal structure of [Fe(II)Mn(II)BPMP($\text{O}_2\text{CCH}_2\text{CH}_3$)₂]BPh₄ (1) has been determined.¹⁶ It shows an iron and a manganese atom bridged by the phenolate oxygen atom of BPMP and by two additional propionate ligands to form a triply bridged dinuclear core (Fig. 1). The analogous complexes [Fe(II)Co(II)BPMP($\text{O}_2\text{CCH}_2\text{CH}_3$)₂]BPh₄ (2) and [Fe(II)Zn(II)BPMP($\text{O}_2\text{CCH}_2\text{CH}_3$)₂]BPh₄ (3) are assumed to have similar structures. The proton labels as shown in Fig. 1 are used for all three complexes in the following ¹H NMR assignments.

The ¹H NMR spectra of complexes 1, 2 and 3 consist of relatively sharp resonances that span over 200 ppm in chemical shifts (Fig. 2). The high resolution and the relatively narrow linewidths observed in the spectra are as expected for the high-spin Fe(II) complexes.²⁰ Unlike the Fe(II)Fe(II) complex,^{18,27,31} these three compounds do not have a two-fold axis of symmetry. Consequently, their ¹H NMR spectra exhibit almost twice as many peaks as that of the corresponding Fe(II)Fe(II) complex. Excluding the BPh₄ and residual solvent proton peaks, a typical 1D ¹H NMR spectrum of such a complex should give 37 ¹H NMR resonances: sixteen from the α -, β -, β' - and γ -protons of the four pyridine rings, three from the *meta*- and *para*-methyl protons on the bridging phenolate ring, twelve from the aminomethylene protons of the BPMP ligand and six from the α - and β -protons of the two bridging propionates. Based on peak counting and integration, we found 37 resonances in the spectra of the Fe(II)Co(II) and Fe(II)Zn(II) complexes, but only 33 signals in the spectrum of the Fe(II)Mn(II) complex, the pyridine α resonances being too broad to be observed. The spectra of the Fe(II)Mn(II) and Fe(II)Co(II) complexes show almost no features in the diamagnetic region except for the BPh₄ and residual solvent protons because both metal sites are paramagnetic in these complexes. The spectrum of the Fe(II)Zn(II) complex, on the other hand, exhibits paramagnetically shifted peaks which are associated with the Fe(II) half of the molecule and a number of features in the 0–20 ppm region which are associated with the Zn(II) half and are shifted due to the dipolar effects of the Fe(II) centre. The weak impurity peaks in the spectra of Fe(II)Co(II) and Fe(II)Zn(II) complexes are from homodinuclear species, e.g. Fe(II)Fe(II), Co(II)Co(II) and Zn(II)Zn(II), due to the site scrambling during the recrystallization process. We have tentatively assigned many of the ¹H NMR signals

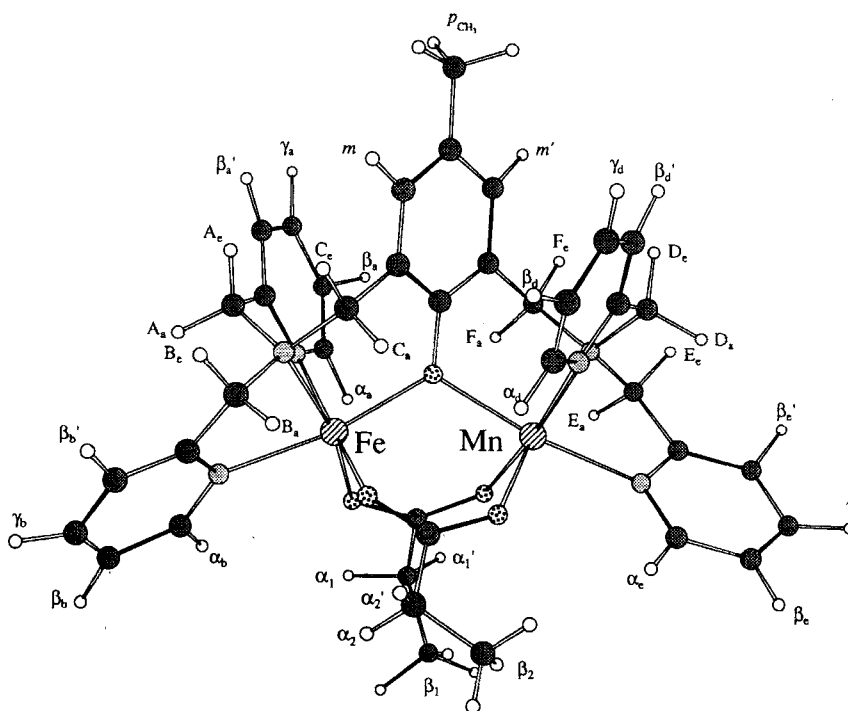


Figure 1. Plot of the structure of $[\text{Fe(II)Mn(II)BPMP}(\text{O}_2\text{CCH}_2\text{CH}_3)_2]^+$ obtained by X-ray crystallography. All the protons are labeled according to their position in the molecule.

on the basis of their chemical shifts, integrations and T_1 values, through bond connectivities from COSY data and by analogy to the assignments made for the corresponding Fe(II)Fe(II) complexes.^{18,27}

The β - and γ -protons on the pyridine rings of the ligand BPMP and the α - and β -protons on the bridging propionates give rise to relatively sharp features which make it possible to establish the bond connectivities among those protons through 2D NMR experiments. In a COSY experiment, the signal from the β -proton of a pyridyl ring shows a cross peak to the signal from its neighbouring γ -proton, which in turn shows a cross peak to the signal from the other β -proton (the β' -proton) on the same ring. Also, the signals from the two diastereotopic α -protons of each bridging propionate show a cross peak between each other and cross peaks to the signal from the β -methyl protons. ^1H COSY spectra of the Fe(II)Mn(II), Fe(II)Co(II) and Fe(II)Zn(II) complexes are shown in Figs 3, 4 and 5, respectively. For 1 and 2, 14 cross peaks are observed in each COSY map, from which the β - γ - β' connectivities for all the four pyridines (two cross peaks each) and the α - β connectivities for the two bridging propionates (three cross peaks each) can be established. For 3, 10 cross peaks can be observed in the 0–60 ppm region from the paramagnetically shifted signals (Fig. 5), four of which come from the β - γ - β' connectivities for the two pyridines (two cross peaks each) coordinated to the paramagnetic Fe(II) site and six of which come from the α - β connectivities in the two bridging propionates (three cross peaks each). The remaining cross-peaks are found in the 0–20 ppm region and associated with the diamagnetic Zn(II) half of the molecule. Because of the sharper signals of the pyridine rings coordinated to the Zn(II) site, three cross signals (α - β - γ - β' connectivities) for each pyridine are observed (Fig. 6).

All the broad signals in the Fe(II)Zn(II) case are from the Fe(II) half of the molecule, including six signals from the three aminomethylene proton pairs and the α -protons on the two pyridine rings. The α -pyridine ring protons have the shortest Fe–H distances and thus have the shortest T_1 values, because the T_1 values are proportional to the inverse sixth power of the metal–H distance in a paramagnetic system.¹⁹ They are also strongly shifted downfield. Therefore, they are easily identified (Fig. 2 and Table 1). The different chemical shifts for the geminal proton pairs result from chelate ring formation, which affords different Fe–N–C–H dihedral angles (to make one proton equatorial-like and the other axial-like), resulting in different amounts of spin delocalization. In early studies of diamine complexes of paramagnetic transition metal ions, the geminal methylene protons were found to shift differently with the equatorial-like proton shifted further downfield.³² The equatorial-like protons have longer Fe–H distances and thus show sharper resonances and longer relaxation times than the axial protons. The six aminomethylene protons have been assigned based on this principle and by comparison with the published data for the corresponding Fe(II)Fe(II) complexes;^{18,27} each aminomethylene pair consists of a broad and a sharp signal corresponding to the axial-like (a) and the equatorial-like (e) protons, respectively (Table 1). Unfortunately, the short T_1 values associated with these resonances do not allow the geminal pairs to be correlated in the COSY spectrum. The remaining sharp signals in the 1D ^1H NMR spectrum of 3 (Fig. 2, bottom) come from the bridging phenolate ring and the aminomethylene proton pairs located in the Zn(II) half of the molecule. The *meta*-, *para*-methyl and *meta'*-protons of the bridging phenolate ring can easily be singled out because they are usually downfield shifted and have the

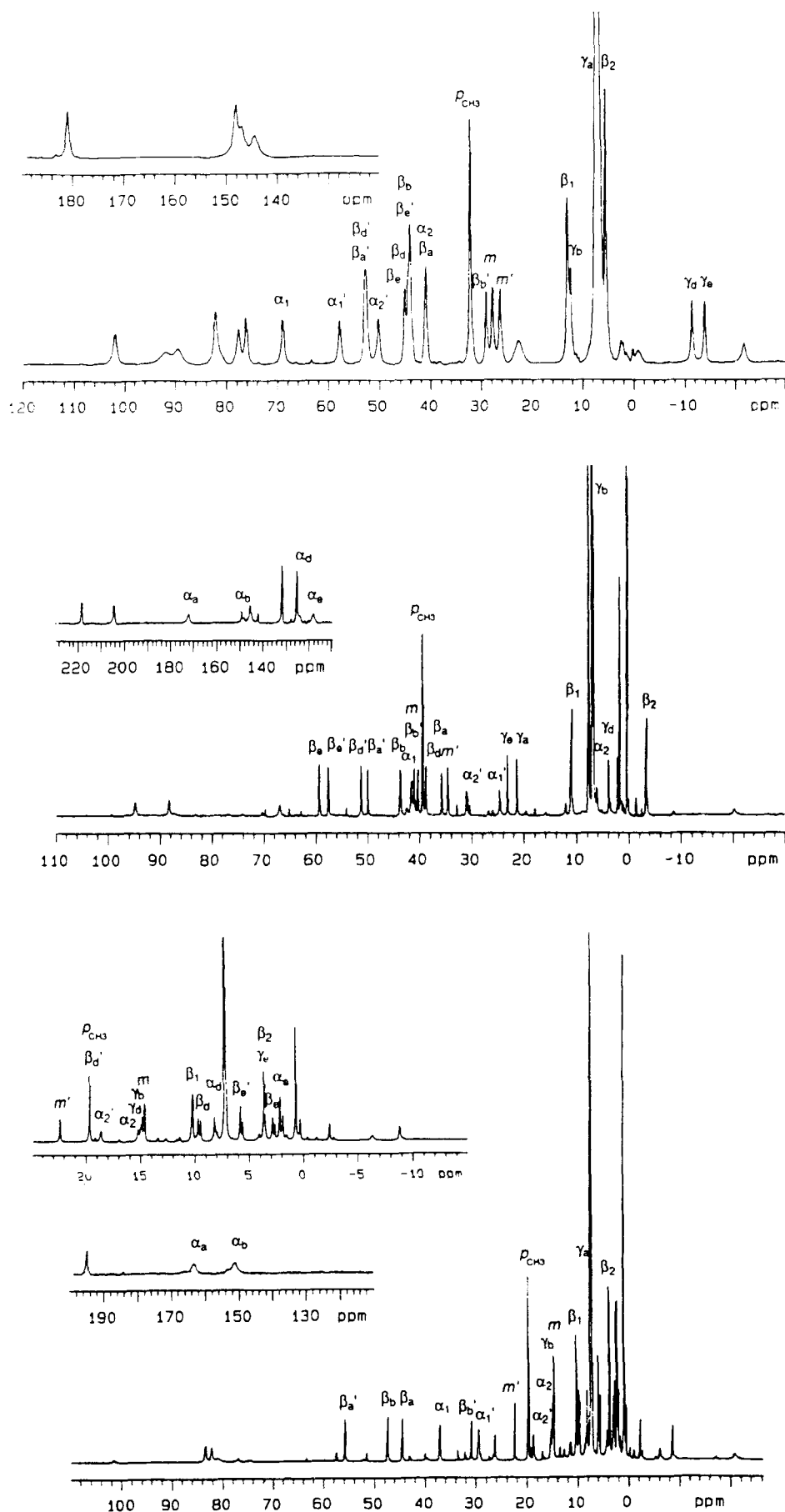


Figure 2. 1D ^1H NMR spectra of $[\text{Fe}(\text{II})\text{Mn}(\text{II})\text{BPMP}(\text{O}_2\text{CCH}_2\text{CH}_3)_2]\text{BPh}_4$ in CD_2Cl_2 (top), $[\text{Fe}(\text{II})\text{Co}(\text{II})\text{BPMP}(\text{O}_2\text{CCH}_2\text{CH}_3)_2]\text{BPh}_4$ in CDCl_3 (middle) and $[\text{Fe}(\text{II})\text{Zn}(\text{II})\text{BPMP}(\text{O}_2\text{CCH}_2\text{CH}_3)_2]\text{BPh}_4$ in CDCl_3 (bottom).

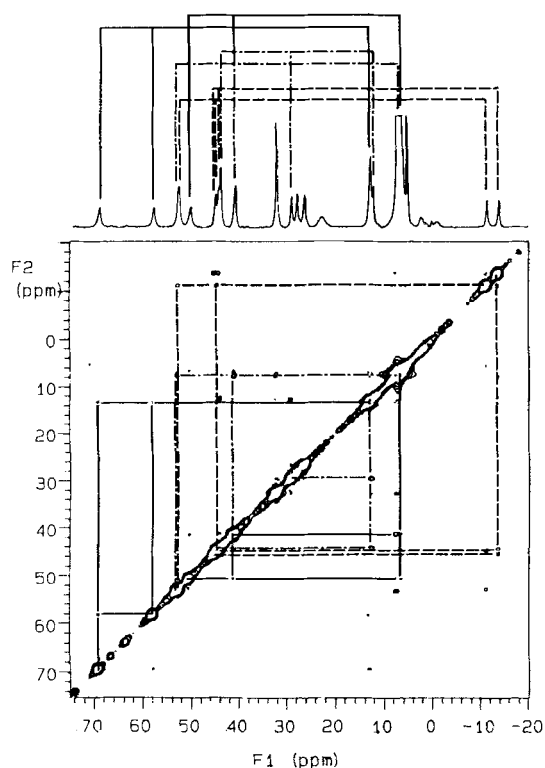


Figure 3. Magnitude mode COSY spectrum of [Fe(II)Mn(II)-BPMP(O₂CCH₂CH₃)₂]BPh₄ in CD₂Cl₂. The COSY spectrum was obtained using 1024(*t*₂) × 256(*t*₁) data points and apodized by the use of a combined sine bell–Gaussian function and zero-filled to afford a 2K(*t*₂) × 2K(*t*₁) matrix which was then Fourier transformed and symmetrized. The assignments are listed in Table 1 and the proton connectivities are shown in the COSY spectrum (---, β–γ–β' connection among the pyridyl protons of the Mn(II) site; ···, β–γ–β' connection the pyridyl protons of the Fe(II) site; and —, α,α'–β connection among the bridging propionate protons). The cross signals at 32.5 and 7.5 ppm are spectrometer artifacts that depend on the setting of the transmitter offset frequency.

integration ratio of 1:3:1 (Fig. 2 and Table 1). There is an additional cross peak observed in Fig. 6 which allows us to identify one of the three aminomethylene pairs in the Zn(II) half of the molecule (Table 1).

Other than establishing bond connectivities, the 2D data alone do not allow us to discriminate between different pyridine rings or the β- and β'-protons on the same ring. However, our proposed assignments of the bond-correlated signals observed in the COSY spectra (Figs 3 and 4) to specific pyridine protons of the Fe(II)Mn(II) and Fe(II)Co(II) complexes have been arrived at by comparing their chemical shifts and *T*₁ values with the results from corresponding Fe(II)Fe(II) complexes^{18,27} and other known data.^{19,20} Specific deuteration would be required to achieve unambiguous assignment.

Assuming that the correlation time is vanishingly small relative to the transition frequencies for the electron (ω_e) and nucleus (ω_i) (fast motion limit, typical of many liquid solutions), the Solomon equation which gives the metal-centred, dipolar contribution to the *T*₁ values is simplified to:

$$T_{1M}^{-1} = \frac{4}{3} \left(\frac{\mu_0}{4\pi} \right)^2 \frac{\gamma_N^2 g_e^2 \mu_B^2 S(S+1) \tau_c}{r^6} = K_M \frac{\tau_c}{r^6} \quad (1)$$

where the constants have their standard values. The spin quantum number of the particular metal centre is denoted as *S*, *r* is the distance from the metal centre to the proton and τ_c is the correlation time. The equation clearly demonstrates that not only does τ_c affect the observed *T*₁ values, but *S* also does so. As shown by the elegant work of Bertini *et al.*³³ on coupled bimetallic complexes, the faster relaxing ion dominates the system electron spin relaxation and thus imposes a common relaxation rate (i.e. correlation time, τ_c) on both metals. The following equation can then be used for the *T*₁ values of the coupled bimetallic complexes:

$$T_1^{-1} = \left(\frac{K'_{M1}}{r_1^6} + \frac{K'_{M2}}{r_2^6} \right) \tau_c \quad (2)$$

where *K*'_{M1} and *K*'_{M2} are the constant values of the respective metal ions shown in Eqn (1) multiplied by an appropriate correction factor to account for the coupling between the two metals, and *r*₁ and *r*₂ are the distances for the proton to the respective metal centres. Hence the coupling interaction between Fe(II) and Mn(II) in 1 give rise to a common electron spin relaxation rate dominated by the faster relaxing Fe(II) centre and permits the observation of the isotropically shifted signals on an Mn(II) complex, a centre that normally gives rise to unobservably broad lines. However, even though the two metals have the same correlation time,

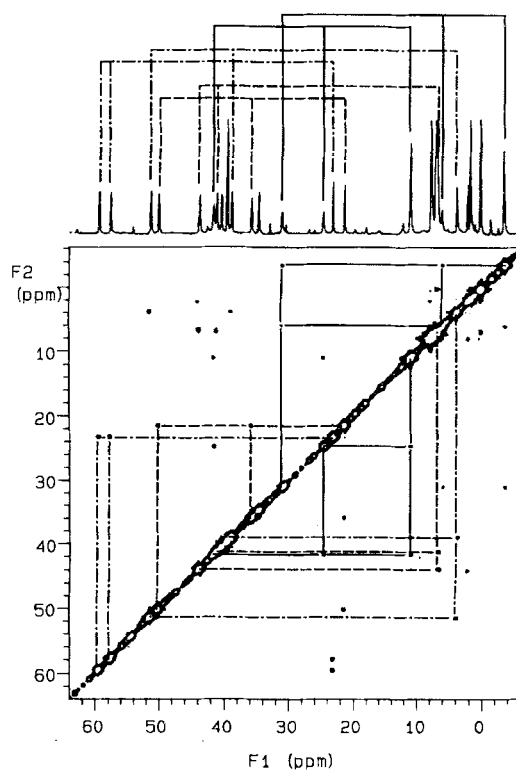


Figure 4. Magnitude mode COSY spectrum of [Fe(II)Co(II)-BPMP(O₂CCH₂CH₃)₂]BPh₄ in CDCl₃. The COSY spectrum was obtained using 1024(*t*₂) × 256(*t*₁) data points and apodized by the use of a combined sine bell–Gaussian function and zero-filled to afford 2K(*t*₂) × 2K(*t*₁) matrix which was then Fourier transformed and symmetrized. The assignments are listed in Table 1 and the proton connectivities are shown in the COSY spectrum (---, β–γ–β' connection among the pyridyl protons of the Fe(II) site; ···, β–γ–β' connection among the pyridyl protons of the Co(II) site; and —, α,α'–β connection among the bridging propionate protons).

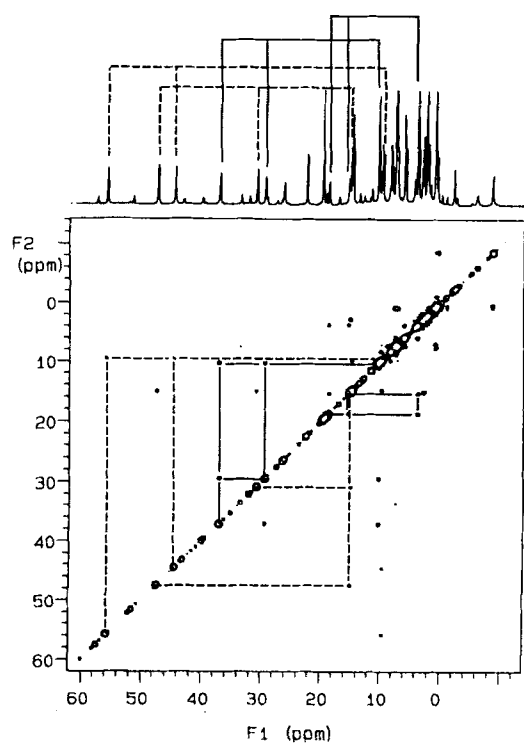


Figure 5. Magnitude mode COSY spectrum of $[\text{Fe(II)Zn(II)BPMP}(\text{O}_2\text{CCH}_2\text{CH}_3)_2]\text{BPh}_4$ in CDCl_3 . The COSY spectrum was obtained using $1024(t_2) \times 256(t_1)$ data points and apodized by the use of a combined sine bell-Gaussian function and zero-filled to afford $2\text{K}(t_2) \times 2\text{K}(t_1)$ matrix which was then Fourier transformed and symmetrized. The assignments are listed in Table 1 and the proton connectivities are shown in the COSY spectrum (---, β - γ - β' connection among the pyridyl protons of the Fe(II) site; and —, α , α' - β connection among the bridging propionate protons).

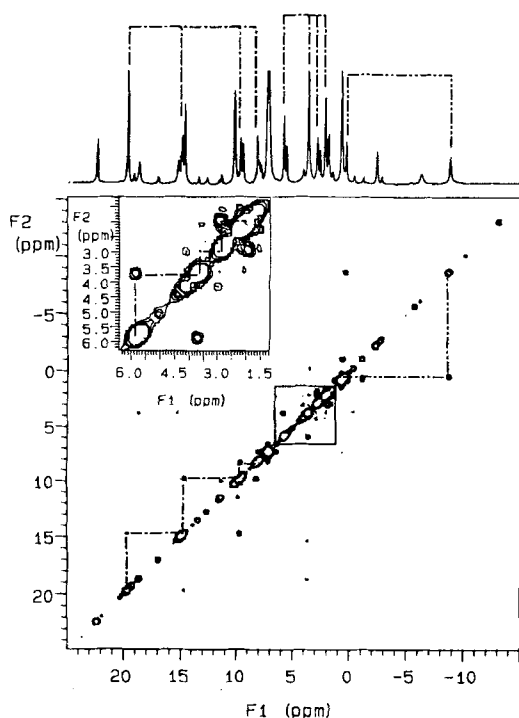


Table 1. NMR assignments of the $[\text{Fe(II)M(II)-BPMP}(\text{O}_2\text{CCH}_2\text{CH}_3)_2]\text{BPh}_4$ complexes

Signals	Fe(II)Mn(II)		Fe(II)Co(II)		Fe(II)Zn(II)	
	δ (ppm)	T_1 (ms)	δ (ppm)	T_1 (ms)	δ (ppm)	T_1 (ms)
α_a	—	—	172.1	0.8	162.8	0.9
β_a	41.3	^a	35.7	10.6	44.6	13.6
γ_a	7.5	^a	21.3	30.7	9.5	34.0
β_a'	53.0	^a	50.0	13.5	55.9	14.8
α_b	—	—	148.7	0.7	150.5	0.8
β_b	44.3	11.3	43.9	11.5	47.4	15.3
γ_b	12.7	22.5	6.8	^a	14.9	37.0
β_b'	29.4	13.4	41.0	9.0	30.8	12.4
A_a	-21.4	1.8	-20.3	1.0	-21.0	1.3
A_e	76.6	3.6	88.4	2.8	83.4	3.6
B_a	23.1	0.7	42.5	1.1	26.2	1.1
B_e	82.6	2.9	94.5	2.6	82.3	2.7
C_a	92.2	0.6	67.0	1.2	81.3	1.0
C_e	181.3	3.1	204.2	2.5	194.5	2.7
α_d	—	—	124.5	^a	8.2	99
β_d	44.8	9.2	38.8	17.9	9.7	96
γ_d	-11.1	15.9	3.8	36.0	15.0	82
β_d'	53.0	8.8	51.2	17.7	19.7	109
α_e	—	—	118.7	0.9	2.2	95.0
β_e	45.4	9.4	59.3	19.6	2.9	92.3
γ_e	-13.6	17.3	23.1	38.2	3.7	^a
β_e'	44.3	11.3	57.5	16.5	5.9	100.0
D_a	90.0	0.7	12.3	2.3	-2.3	20.1
D_e	78.1	2.4	137.0	6.4	2.7	62.4
E_a	144.9	0.9	-1.5	3.1	1.9	22.3
E_e	102.3	2.1	125.2	5.0	5.7	61.0
F_a	147.5	1.3	145.0	1.7	-8.8	15.2
F_e	148.4	1.9	218.0	3.8	0.4	46.1
m	28.2	10.8	40.3	13.5	14.7	27.0
p_{CH_3}	32.5	43.0	39.5	61.3	19.7	109
m'	26.7	9.5	34.6	15.7	22.4	38.9
α_1	69.4	3.7	41.6	4.9	37.1	9.7
α_1'	58.2	3.5	24.6	4.8	29.5	8.7
β_1	13.3	6.7	11.0	9.1	10.3	14.0
α_2	41.3	4.7	6.1	6.7	15.3	8.3
α_2'	50.6	4.1	31.0	5.2	18.7	6.8
β_2	6.3	^a	-3.4	9.8	3.8	27.5

^a Signal not resolved.

they will impart different relaxation rates on the protons owing to their different spin quantum numbers. The large spin on Mn(II) imparts a shorter T_1 [Eqn (1)] at a comparable distance than Fe(II) and affords broader lines for the Mn(II) half of the complex. This effectively separates the Fe(II)Mn(II) complex into an Fe(II) 'side' and an Mn(II) 'side.' By analogy, the Fe(II)Co(II) molecule can also be separated into an Fe(II) 'side' and a Co(II) 'side.' Based on the above theory and the bond connectivity patterns observed in the COSY maps, the pyridine ring protons for **1** and **2** were assigned (Fig. 2 and Table 1). The relatively sharp

Figure 6. Magnitude mode COSY spectrum of the diamagnetic region of $[\text{Fe(II)Zn(II)BPMP}(\text{O}_2\text{CCH}_2\text{CH}_3)_2]\text{BPh}_4$ in CDCl_3 . The COSY spectrum was obtained using $1024(t_2) \times 256(t_1)$ data points and apodized by the use of a combined sine bell-Gaussian function and zero-filled to afford $2\text{K}(t_2) \times 2\text{K}(t_1)$ matrix which was then Fourier transformed and symmetrized. The assignments are listed in Table 1 and the proton connectivities are shown in the COSY spectrum (---, α - β - γ - β' connection among the pyridyl protons of the Zn(II) site; - · · ·, connection between two methylene protons).

signals remaining are then associated with those on the phenolate bridge, which are easily singled out and assigned based on their integrations (Table 1). The broad signals from the aminomethylene protons (twelve each) in **1** and **2** and the α -protons of the four pyridine rings in **2** are assigned as discussed for **3** (Table 1).

Table 1 lists all the assignments we have made so far for the ^1H NMR resonances from all the protons except the BPh_4 and the solvent protons in the three complexes. The assignments for the proton resonances from the four distinct pyridine rings and the bridging phenolate ring in the BPMP ligand and those from the two bridging propionates in each of the three complexes are unambiguous because of the bond-correlated cross signals observed in the COSY spectra and their relaxation behaviour (T_1 values). However, the assignments for the aminomethylene proton resonances are more tentative because they are solely based on a comparison of the proton configurations in the molecule and the T_1 values. We also attempted NOESY and TOCSY experi-

ments on these complexes, but we were unable to obtain NOESY cross signals and the TOCSY map was essentially identical to the COSY map.

This work demonstrates that 2D COSY techniques can be performed on paramagnetic bimetallic mixed-metal complexes. All the through-bond cross signals arising from the relatively sharp resonances (with T_1 values >3 ms) can be observed in just one COSY experiment. In combination with T_1 measurements, reasonable assignments can be made for all the proton NMR signals of the Fe(II)Mn(II) , Fe(II)Co(II) and Fe(II)Zn(II) complexes.

Acknowledgements

This work was supported by the National Institutes of Health Grant GM-38767. T.R.H. was a recipient of a Doctoral Dissertation Fellowship from the Graduate School of the University of Minnesota. The Varian NMR spectrometers were purchased from funds provided by the National Institutes of Health, National Science Foundation and the University of Minnesota. We thank Drs Li-June Ming and Vikram Roongta for valuable input.

REFERENCES

1. L. Que, Jr, and A. E. True, *Prog. Inorg. Chem.* **38**, 97 (1990).
2. P. C. Wilkins and R. G. Wilkins, *Coord. Chem. Rev.* **79**, 195 (1987).
3. P. Reichard and A. Ehrenberg, *Science (Washington, DC)* **221**, 514 (1983).
4. B. G. Fox, K. K. Surerus, E. Münck and J. D. Lipscomb, *J. Biol. Chem.* **263**, 10553 (1988).
5. B. C. Antanaitis and P. Aisen, *Adv. Inorg. Biochem.* **5**, 111 (1983).
6. B. A. Averill, J. C. Davis, S. Burman, T. Zirino, J. Sanders-Loehr, T. M. Loehr, J. T. Sage and P. G. Debrunner, *J. Am. Chem. Soc.* **109**, 3760 (1987).
7. B. G. Fox, J. Shanklin, C. Somerville and E. Münck, *Proc. Natl. Acad. Sci. USA* **90**, 2486 (1993).
8. D. T. Keough, D. A. Dionysius, J. de Jersey and B. Zerner, *Biochem. Biophys. Res. Commun.* **94**, 600 (1980).
9. J. C. Davis and B. A. Averill, *Proc. Natl. Acad. Sci. USA* **79**, 4623 (1982).
10. J. L. Beck, D. T. Keough, J. de Jersey and B. Zerner, *Biochim. Biophys. Acta* **791**, 357 (1984).
11. S. S. David and L. Que, Jr, *J. Am. Chem. Soc.* **112**, 6455 (1990).
12. R. C. Holz, L. Que, Jr, and L.-J. Ming, *J. Am. Chem. Soc.* **114**, 4434 (1992).
13. M. Suzuki, H. Kanatomi and I. Murase, *Chem. Lett., Chem. Soc. Jpn.* **54**, 1745 (1981).
14. A. S. Borovik, V. Papaefthymiou, L. F. Taylor, O. P. Anderson and L. Que, Jr, *J. Am. Chem. Soc.* **111**, 6183 (1989).
15. T. R. Holman, C. Juarez-Garcia, M. P. Hendrich, L. Que, Jr, and E. Münck, *J. Am. Chem. Soc.* **112**, 7611 (1990).
16. T. R. Holman, PhD Thesis, University of Minnesota (1991).
17. T. R. Holman and L. Que, Jr, unpublished results.
18. A. S. Borovik, M. P. Hendrich, T. R. Holman, E. Münck, V. Papaefthymiou and L. Que, Jr, *J. Am. Chem. Soc.* **112**, 6031 (1990).
19. G. N. La Mar, W. DeW. Horrocks, Jr, and R. H. Holm (Eds), *NMR of Paramagnetic Molecules, Principles and Application*. Academic Press, New York (1987).
20. I. Bertini and C. Luchinat, *NMR of Paramagnetic Molecules in Biological Systems*. Benjamin/Cummings, Menlo Park, CA (1986).
21. R. R. Ernst, G. Bodenhausen and A. Wokaun, *Principle of Nuclear Magnetic Resonances in One and Two Dimensions*. Oxford University Press, Oxford (1987).
22. W. Peters, M. Fuchs, H. Sicius and W. Kuchen, *Angew. Chem., Int. Ed. Engl.* **24**, 231 (1985).
23. B. G. Jenkins and R. B. Lauffer, *Inorg. Chem.* **27**, 4730 (1988).
24. B. G. Jenkins and R. B. Lauffer, *J. Magn. Reson.* **80**, 328 (1988).
25. C. Luchinat, S. Steuernagel and P. Turano, *Inorg. Chem.* **29**, 4351 (1990).
26. K. A. Keating, J. S. deRopp, G. N. La Mar, A. L. Balch, F. Y. Shiau and K. M. Smith, *Inorg. Chem.* **30**, 3258 (1991).
27. L.-J. Ming, H. G. Jang, and L. Que, Jr, *Inorg. Chem.* **31**, 359 (1992).
28. L. P. Liu, G. N. La Mar and K. Rajarathnam, *J. Am. Chem. Soc.* **112**, 9527 (1990).
29. J. S. deRopp, G. N. LaMar, W. Wariishi and M. H. Gold, *J. Biol. Chem.* **266**, 15001 (1991).
30. L. Banci, I. Bertini, P. Turano, M. Tien and T. K. Kirk, *Proc. Natl. Acad. Sci. USA* **88**, 6956 (1991).
31. H. G. Jang, M. P. Hendrich and L. Que, Jr, *Inorg. Chem.* **32**, 911 (1993).
32. R. H. Holm and C. J. Hawkins, in *NMR of Paramagnetic Molecules, Principles and Applications*, edited by G. N. La Mar, W. DeW. Horrocks, Jr, and R. H. Holm, Chapt. 7. Academic Press, New York (1987).
33. I. Bertini, C. Owens, C. Luchinat and R. S. Drago, *J. Am. Chem. Soc.* **109**, 5208 (1987).